

Cryptococcal Choroid Plexitis as a Mass Lesion: MR Imaging and Histopathologic Correlation

Jerry M.E. Koor, Anita Mahadevan, Jayakumar P. Narayan, Srikanth S. Govindappa, P. Satishchandra, Anisya V. Taly, and S. K. Shankar

Summary: Cryptococcosis is a relatively common mycotic infection of the CNS caused by a ubiquitous saprophytic fungus. We present an unusual case of CNS cryptococcosis in an immunocompetent patient. Florid choroid plexitis resulted in the formation of intraventricular enhancing mass lesions that filled the ventricles and were hyperintense to associated periventricular edema on T2-weighted MR images. We also noted lesions corresponding to microcystic, dilated Virchow-Robin spaces in the basal ganglia that were characteristic of cryptococcal infection.

Cryptococcus neoformans is the most common fungus to affect the CNS and to cause meningoencephalitis. Although the incidence of cryptococcal infection is high when associated with HIV infection or AIDS, this infection can occur in an immunocompetent, healthy host as well. The pathogenesis of this infection is remarkably similar to that of tuberculous meningitis in hematogenous route to the CNS from a peripheral focus in the lung. A choroid plexitis causing an intraventricular mass lesion with entrapment and dilatation of the ventricle is distinctly unusual. To our knowledge, a solitary case of cryptococcal choroid plexitis has been described in the literature (1). We present the CT and MR imaging features of such an infection in an immunocompetent patient and correlate these with pathologic findings at autopsy.

Case Report

A previously healthy 44-year-old man had an insidious onset of left lower-limb weakness of 2 months' duration. He also had memory loss, failed to recognize his relatives, and had difficulty finding his way around his home. He was dull and apathetic with social disinhibition and urinary incontinence. He complained of occasional episodes of projectile vomiting and giddiness that were associated with blurred vision over 2 to 3 months. Two days before coming to the hospital, he had totally lost the ability to speak. A cranial CT scan obtained at another

hospital revealed a communicating hydrocephalus, on which basis a provisional diagnosis of tuberculous meningitis was made. He underwent antituberculous therapy for 1 month, with no perceptible effect.

At admission, the patient was unresponsive to oral commands and moved only his right-sided limbs in response to painful stimuli. He had neck stiffness, brisk deep-tendon reflexes on the left side, and bilateral equivocal plantars. Ocular movements and fundi were normal. Examination of the ventricular CSF showed 15 lymphocytes per mm³, 1.47 g/dL protein, and 35 mg/dL glucose. India-ink preparation of CSF was positive for cryptococci. Repeat CSF examination after 7 weeks showed an increase in protein to 2.9 g/dL, 22 mg/dL glucose, and nil cells. Immune complexes to mycobacterium (IgG type) were detected in the CSF. He underwent CT and MR imaging examinations (Fig 1).

The patient received treatment for cryptococcal meningitis in addition to antituberculous therapy. His sensorium improved over the next 4 weeks, but he developed bedsores, sepsis, and electrolyte imbalances (hyponatremia and hypokalemia). Blood cultures yielded findings of *Pseudomonas aeruginosa* and *Staphylococcus epidermidis*. Urine cultures grew *Staphylococcus aureus* and nonhemolytic streptococci. He received appropriate antibiotics after establishing antibiotic sensitivity. Serum tests for HIV antibodies were nonreactive (negative) twice. The absolute CD4 cell count was 1540 mm³ (laboratory normal range, 290–2600 per mm³). Antifungal therapy was monitored by repeated lumbar CSF examination for cryptococci, which continuously manifested positive findings, and cryptococci were cultured from the CSF. The patient showed substantial improvement in his sensorium over the next 3 months. Routine hematologic and biochemical parameters of the blood were stable, although the level of protein in the CSF remained high, indicating blockage of the CSF pathways. His condition worsened, and 95 days after admission, he died.

Partial autopsy confined to examination of the brain was conducted 5 hours after death by use of histologic examination (Figs 2 and 3). The brain was encased in a thick, mucinous exudate that covered the surface and the basal cisterns, ensheathing the cranial nerves at the base. The choroid plexus at both foramina of Lushka was infiltrated to form nodular, mucoid masses in the cerebellopontine angle. Similar mucoid masses also filled the third ventricle, blocking the foramen of Munro on both sides (Fig 2A and B), the trigone of the lateral ventricle, and the left temporal horn (Fig 2). The lesion trapped the frontal and occipital horns of the lateral ventricle; a few loculated spaces were spared. At microscopic examination, numerous actively budding cryptococcal cysts were seen floating in pools of mucin (Fig 3).

The corona radiata, body of the corpus callosum, head of the caudate nucleus, internal capsule, and putamen on both sides had microcystic parenchymal lesions. These corresponded histologically to distended Virchow-Robin spaces filled with budding cryptococci that compressed the vascular lumina. The periventricular white matter was diffusely edematous and revealed demyelination corresponding to the periventricular hyperintensities noted on MR images. The brain stem was en-

Received March 7, 2001; accepted after revision July 26.

From the Departments of Neuroimaging and Interventional Radiology (J.M.E.K., J.P.N., S.S.G.), Neuropathology (A.M., S.K.S.), and Neurology (P.S., A.V.T.), National Institute of Mental Health and Neurosciences, Bangalore, India.

Presented at the 16th Annual Karnataka State Conference of the Indian Radiological and Imaging Association, Bangalore, India.

Address reprint requests to Prof. P.N. Jayakumar, Head of Department of Neuroimaging and Interventional Radiology, National Institute of Mental Health and Neurosciences, Bangalore 560 029, India.

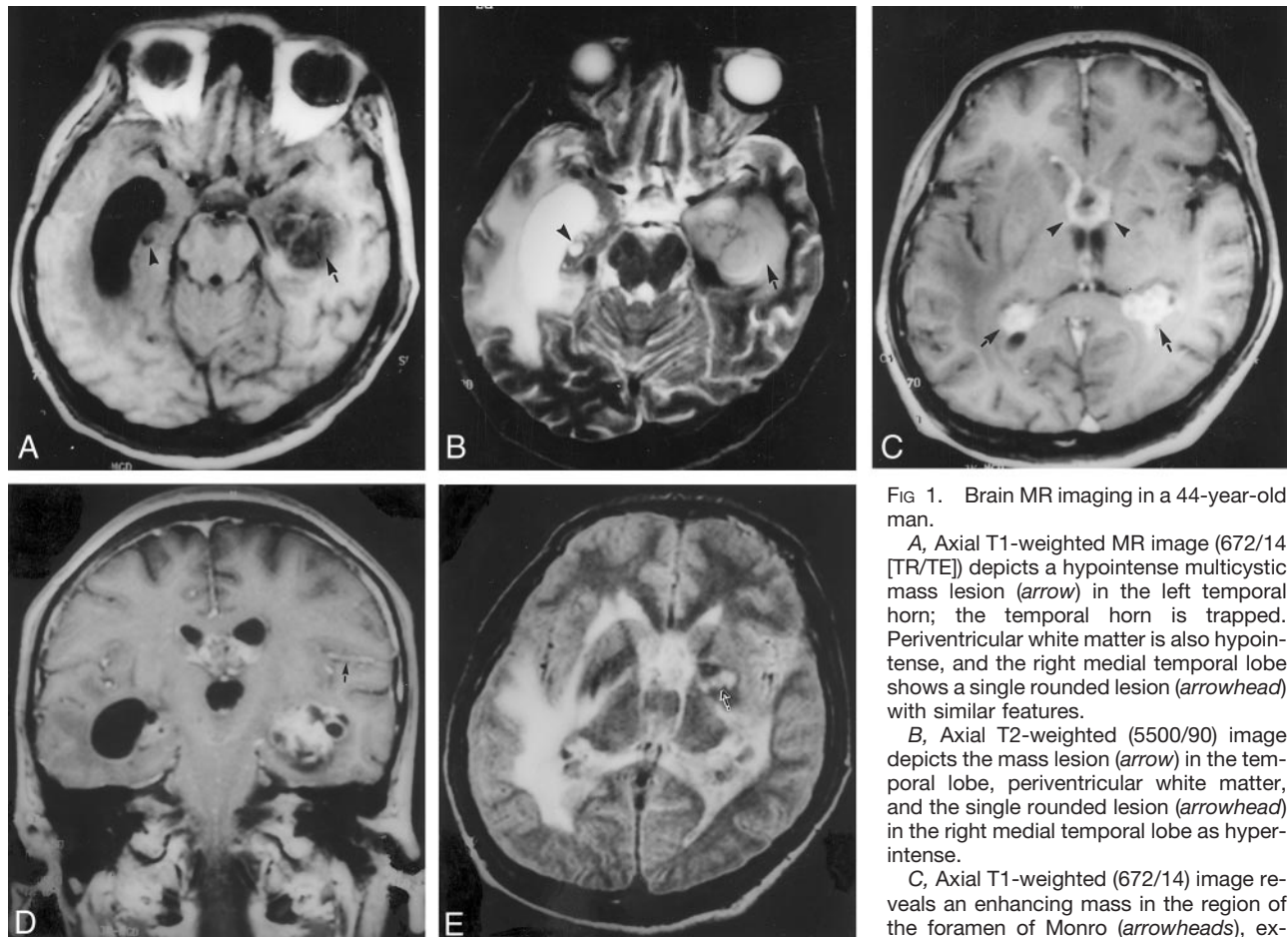


FIG 1. Brain MR imaging in a 44-year-old man.

A, Axial T1-weighted MR image (672/14 [TR/TE]) depicts a hypointense multicystic mass lesion (arrow) in the left temporal horn; the temporal horn is trapped. Periventricular white matter is also hypointense, and the right medial temporal lobe shows a single rounded lesion (arrowhead) with similar features.

B, Axial T2-weighted (5500/90) image depicts the mass lesion (arrow) in the temporal lobe, periventricular white matter, and the single rounded lesion (arrowhead) in the right medial temporal lobe as hyperintense.

C, Axial T1-weighted (672/14) image reveals an enhancing mass in the region of the foramen of Monro (arrowheads), extending bilaterally into the frontal horns.

Choroid plexuses are enlarged and enhanced (arrow).

D, Coronal T1-weighted (672/14) image shows enhancement of the meninges (arrow).

E, Axial fluid-attenuated inversion recovery (9000/119) image reveals dilated hyperintense Virchow-Robin spaces (arrow) in the basal ganglia.

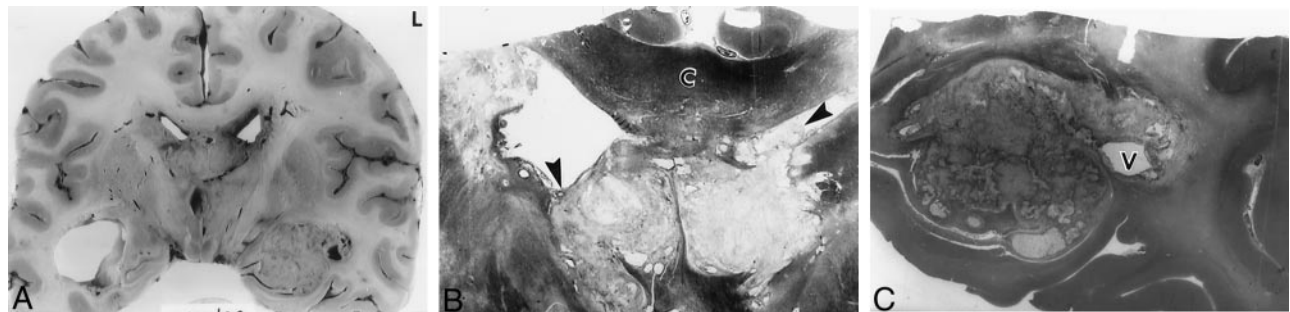


FIG 2. Examination of the brain 5 hours after death.

A, Coronal section of the brain through mammillary bodies shows a mass filling the superior part of the anterior third ventricle, totally blocking both foramina of Munro, and a similar mass plugging the left temporal horn.

B, Whole-mount section through the third ventricle shows a multicystic, pale mass of cryptococci adhering to the corpus callosum (C) and obliterating the foramina of Munro (arrowheads). Note the ragged ventricular lining. Myelin stain, magnification $\times 3$.

C, Whole-mount section through the left temporal horn shows a multicystic cryptococcal mass filling the left temporal horn, sparing only a small area of the ventricle (V). The surrounding white matter is pale because of edema and demyelination. Myelin stain, magnification $\times 2$.

cased by the exudate with a variable mononuclear and giant-cell reaction.

Discussion

The choroid plexus lies at the interface between the cerebrospinal fluid and the systemic circulation, where it

forms an important portal of entry for many infectious agents, including free and even intracellular viruses such as HIV (2). The papillary fronds of the choroid plexus that protrude into the ventricle have an external epithelial lining that is continuous with the ependyma and encloses a vascularized mesenchy-



FIG 3. Microphotograph showing cryptococci (arrowheads) floating in a mucoid background in the Virchow Robin space surrounding a vessel (V). Hematoxylin-eosin stain, magnification $\times 300$.

mal core. In contrast to the tight junctions in the parenchymal capillaries of the CNS, the capillaries of the choroid plexus have gap junctions that place it outside the blood-brain barrier (3). The stroma within the connective-tissue core recently has been shown to contain a network of dendritic cells that express class II molecules of the major histocompatibility complex, which play an important role in immune surveillance (2). Thus, the histologic makeup and strategic location of the choroid plexus make it an important site of initial dissemination for many infectious agents, including those causing tuberculosis, cytomegalovirus, cryptococcosis, and a variety of bacteria and parasites. The choroid plexus is also the seat of noninfectious inflammatory disorders, such as sarcoidosis, xanthogranulomas, and rheumatoid nodules (1). Most intracranial infections that cause meningitis therefore are thought to start in the choroid plexus of the ventricles (4). However, usually the associated encephalitis, meningitis, or ependymitis rather than the choroid plexitis alone (1) causes clinical manifestations.

The method of spreading to the CNS for most infectious agents is through hematogenous dissemination. The pathogenesis of cryptococcal infection has many similarities to that of tuberculosis. Infection is acquired through inhalation in both disease conditions, and once inhaled, is contained at the level of the lungs or lymph nodes, where the pathogen can remain dormant. Microorganism proliferation leading to disease occurs only with an encapsulated strain,

with an infective dose so large that the host defenses are overwhelmed, or in the presence of an underlying disease that has crippled host defenses.

In neurotuberculosis, akin to the Ghon's focus in the lung, the subependymal Rich's focus in the CNS forms the primary focus, which can rupture into the ventricle to discharge the bacilli into the CSF to cause meningitis. Similarly, in cryptococcosis, the fungus may reach the choroid plexus by hematogenous spread, colonizing it and subsequently discharging into the CSF to cause meningitis, encephalitis, or ependymitis. The cryptococci also extend into the parenchyma through the Virchow-Robin spaces, and expansion within these spaces forms the pseudocystic lesions characteristic of this disease. Choroid plexitis most often is asymptomatic; the leptomeningeal involvement is responsible for the clinical manifestations of CNS cryptococcosis.

The CNS is a preferred site for cryptococcal infection, because soluble anticryptococcal factors present in serum are absent in CSF (5). The polysaccharide capsule of the fungus hinders phagocytosis and impairs leukocyte migration. Hence, the inflammatory response it evokes is minimal in contrast to other forms of neuroinfections, such as neurotuberculosis. The organism also does not release any exotoxin and thus causes little tissue necrosis. Therefore, secondary changes such as fibrosis, calcification, infarction, or hemorrhage are rare and are caused by compression of the surrounding structures as the infective focus enlarges.

The diagnosis of neuroinfections by imaging studies has long been a challenge to radiologists. The spectrum of MR and CT abnormalities described in CNS cryptococcosis ranges from no abnormality to meningeal enhancement, ventriculomegaly, and meningoencephalitis in the form of either pseudocysts in the basal ganglia or granulomatous lesions. The avascular pseudocysts are seen as well circumscribed, round to oval hypointensities on T1-weighted images and hyperintensities on T2-weighted images, which fail to enhance after administration of contrast medium. These are believed to represent dilated Virchow-Robin spaces filled with budding cryptococci enmeshed within a gelatinous material. Granulomatous lesions enhance at contrast medium administration and are hyperintense on T2-weighted images. They are located preferentially on the ependyma of choroid plexus (6). Because CT and MR imaging findings may be normal in immunocompromised patients, the diagnosis frequently relies on identification of the cryptococci by India-ink preparation or by detection of cryptococcal antigen in CSF. Tien et al (7) suggested that imaging findings differ between immunodeficient and immunocompetent individuals with CNS cryptococcosis. In a series of 29 HIV-positive patients with cryptococcosis, 76% had normal features or cortical atrophy on images, and meningeal enhancement was rare, although meningitis is the most common form of CNS involvement. Meningeal involvement often is inferred from the progressive ventriculomegaly on sequential images, but neither

meningeal enhancement nor ventricular dilatation is specific for cryptococcosis.

The presence of cystic lesions in the basal ganglia on images strongly suggests cryptococcal infection (Fig 1E) (7–9). Cryptococcosis rarely appears as a unilateral or bilateral enlargement of the choroid plexus that enhances at contrast medium administration (6, 10, 11), similar to the present case (Fig 1C), and therefore choroid plexus involvement may be a diagnostic clue. Choroid plexus enhancement is not unique to cryptococcosis; however, it can occur with a variety of lesions, including tuberculosis, cytomegalovirus meningoencephalitis, pyogenic and granulomatous infections, parasitic infestations, and even neoplasms (12). Okuda et al (13) described a case of tuberculous choroid plexitis in which the intense inflammatory reaction readily spread to the ventricular wall, resulting in severe edema of the surrounding brain parenchyma. Purulent ventriculitis, cytomegalovirus meningoencephalitis, and neoplastic lesions such as lymphomas and germinomas, by virtue of their subependymal location and spread, can cause ventricular enhancement, but none of these conditions are associated with the presence of cystic lesions within the basal ganglia. Contrast enhancement of the choroid plexus does not occur in the presence of impaired immunity (14), suggesting that choroidal inflammation is responsible for enhancement and hypointensities on MR images. Periventricular edema (Fig 1A, B, and E) appears to result from altered CSF dynamics and seeping of the CSF into the interstitial space across the subependymal gliotic layer.

Few neuroimaging features of mass lesions caused by choroid plexus involvement, as seen in this case (Fig 1C), have been reported (15–17). Histologic correlation is available from only one report (6), in which the authors describe granulomas in reaction to the fungi. Choroidal inflammation also can cause intraventricular synechiae and loculation (11) or enlargement and entrapment of the temporal horns due to obstruction of free CSF flow by cryptococci (Fig 1A and B). Both forms of choroid plexus involvement were seen in the case reported herein. Although these

findings can occur with any intraventricular lesion, including neoplasms, the combination of strong enhancement of the choroid plexus with cystic lesions within the basal ganglia and meningeal enhancement suggests the diagnosis of CNS cryptococcosis.

References

1. Cho IC, Chang KH, Kim YH, Kim SH, Yu IK, Han MH. **MR features of choroid plexitis.** *Neuroradiology* 1998;40:303–307
2. Hanly A, Petito CK. **HLA-DR reactive dendritic cells of the human choroid plexus: a potential reservoir of HIV in the central nervous system.** *Hum Pathol* 1998;29:88–93
3. Davis DA, Milhorat TH. **The blood brain barrier of the rat choroid plexus.** *Anat Rec* 1975;181:779–790
4. Netsky MG, Shuangshoti S. **The Choroid Plexus in Health and Disease.** Charlottesville, Va: University of Virginia Press; 1975:249–264
5. Igel HJ, Bolande RP. **Humoral defense mechanisms in cryptococcosis: substances in normal human serum, saliva and CSF affecting the growth of *Cryptococcus neoformans*.** *J Infect Dis* 1966;116:75
6. Andreula CF, Burdi N, Carella A. **CNS cryptococcosis in AIDS: spectrum of MR findings.** *J Comput Assist Tomogr* 1993;17:438–441
7. Tien RD, Chu PK, Hesslink JR, Duberg A, Wiley C. **Intracranial cryptococcosis in immunocompromised patients: CT and MR findings in 29 cases.** *AJNR Am J Neuroradiol* 1991;12:283–289
8. Wehn SM, Heinz ER, Burger PC, Boyko OB. **Dilated Virchow-Robin spaces in cryptococcal meningitis associated with AIDS: CT and MR findings.** *J Comput Assist Tomogr* 1989;13:756–762
9. Popovich MJ, Arthur RH, Hemer E. **CT of intracranial cryptococcosis.** *AJNR Am J Neuroradiol* 1990;11:139–142
10. Cornell SH, Jacoby CG. **The varied computed tomographic appearance of intracranial cryptococcosis.** *Radiology* 1982;143:703–707
11. Nicholas JP, Erini VM. **MR of choroid plexus involvement in intracranial cryptococcosis.** *J Comput Assist Tomogr* 1993;17:547–550
12. Mathews VP, Smith RR. **Choroid plexus infections: neuroimaging appearances of four cases.** *AJNR Am J Neuroradiol* 1992;13:374–378
13. Okuda S, Murakami N, Ito E, Hashizume Y. **A case of tuberculous meningitis with abnormal contrast enhancement of the choroid plexus on CT and MR.** *Rinsho Shinkeigaku* 1993;33:1090–1093
14. Berkefeld J, Enzensberger W, Lanfermann H. **Cryptococcal meningoencephalitis in AIDS: parenchymal and meningeal forms.** *Neuroradiology* 1999;41:129–133
15. Weenink HR, Bruyn GW. **Cryptococcosis in the nervous system.** In: Vincken PJ, Bruyn GW, eds. *Handbook of Clinical Neurology*, vol 35. Amsterdam: North Holland; 1978; 459–502
16. Garcia CA, Weisberg LA, Lacorte WSJ. **Cryptococcal intracerebral mass lesions: CT-pathological considerations.** *Neurology* 1985;35:731–734
17. Penar PL, Kim J, Chyatte D, Sabshin JK. **Intraventricular cryptococcal granuloma. Report of two cases.** *J Neurosurg* 1988;68:145–148